ACS NANO

www.acsnano.org

ARTICLE

High-Performance Cold Cathode X-ray Tubes Using a Carbon Nanotube Field Electron Emitter

Jun Soo Han,[§] Sang Heon Lee,[§] Hanbin Go, Soo Jin Kim, Jun Hong Noh, and Cheol Jin Lee*

Cite This: *ACS Nano* 2022, 16, 10231−10241

Read Online

ACCESS | Metrics & More | Article Recommendations | Supporting Information

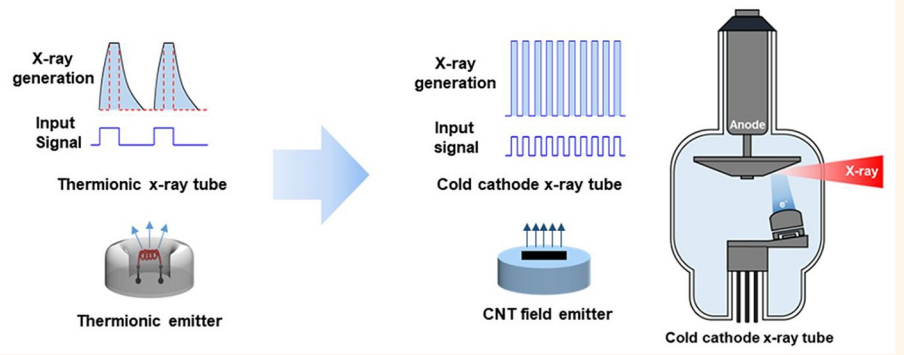

ABSTRACT: **A cold cathode X-ray tube was fabricated using a carbon nanotube (CNT) field electron emitter made by a free-standing CNT film which is composed of a highly packed CNT network. A lot of CNT bundles with a sharp tip are vertically aligned at the edge of the thin CNT film with a length of 10 mm and a thickness of 7 μm. The cold cathode X-ray tube using the CNT field emitter presents an extremely high tube current density of 152 A/cm^2 (corresponding to tube current of 106.4 mA), the electron beam transmittance of 95.2% and a small focal spot size (FSS) of 0.5 mm. In addition, the cold cathode X-ray tube also shows stable lifetime during 100 000 shots. High emission current density of the cold cathode X-ray tube is mainly attributed to a lot of electron emission sites at an edge of the CNT film. The small FSS is caused by an ensemble of the CNT field electron emitter made by a free-standing thin CNT film and the optimized curve-shape elliptical focusing lens. Based on obtained results, the cold cathode X-ray tube can be widely used for various X-ray applications such as medical diagnosis systems and security check systems in the future.**

KEYWORDS: *carbon nanotube, field electron emitter, cold cathode X-ray tube, emission current, emission current density, emission stability, focal spot size*

The demand for medical devices for diagnostic imaging greatly increases as the need for healthcare prevention and diagnosis draws increasing attention. Among various medical diagnostic equipment, X-ray medical systems such as mobile X-ray radiography systems and X-ray CT (computed tomography) systems have assumed an important role in the detection of several diseases, because of the numerous advantages of X-ray imaging techniques. To achieve precise detection of various diseases, X-ray systems require a high-resolution X-ray image at a small X-ray dose as possible. Thermionic X-ray tubes based on a hot-filament tungsten emitter are mostly used in medical X-ray systems until now. By the way, the thermionic X-ray tubes cannot avoid rising time and falling time during X-ray generation, resulting in unnecessary X-ray irradiation. Moreover, they need a high X-ray dose to get a high resolution X-ray images. Therefore, a new X-ray tube that overcomes the limitation of conventional thermionic X-ray tubes remains an unmet challenge in X-ray technology.

Recently, a cold cathode X-ray tube has much attention due to possibility of several advantages such as a high resolution,

Received: March 4, 2022
Accepted: June 8, 2022
Published: June 10, 2022

https://doi.org/10.1021/acsnano.2c02233
ACS Nano 2022, 16, 10231−10241

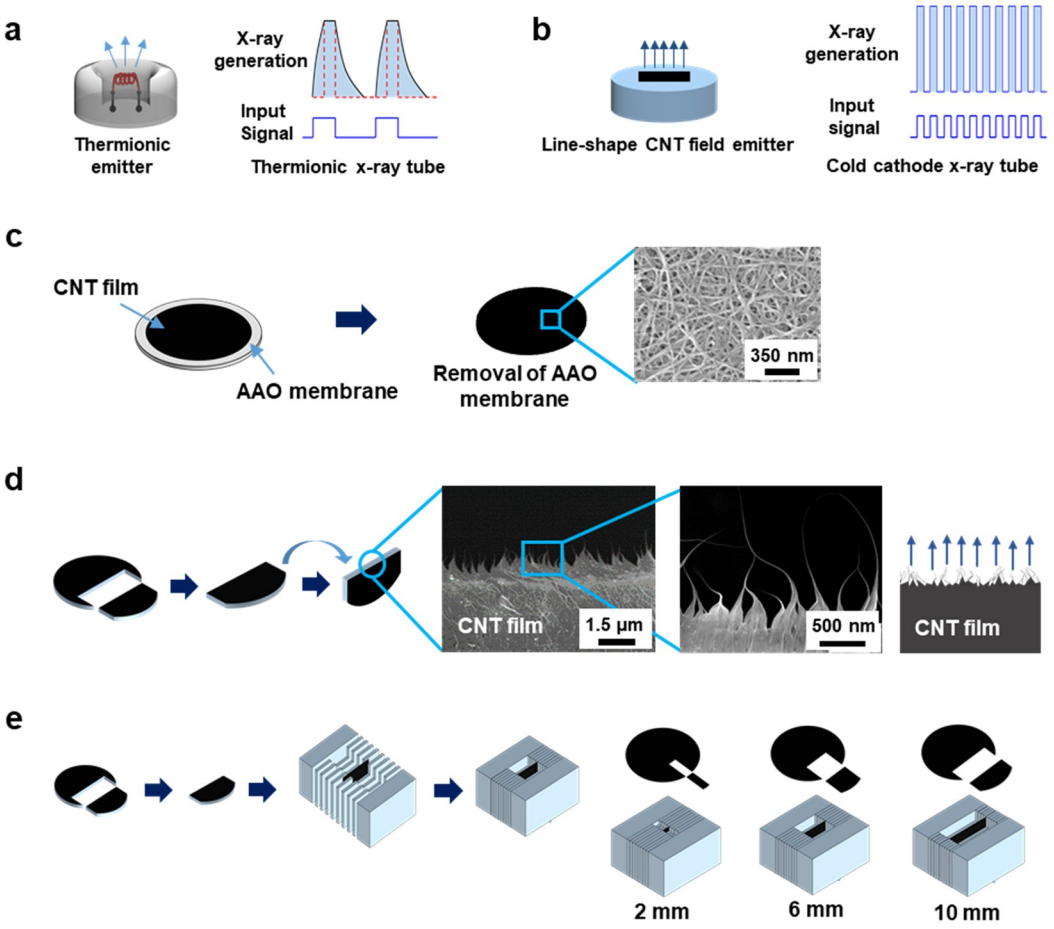

Figure 1. Fabrication of the CNT field electron emitter using a free-standing SWCNT film. (a) Schematics of a filament thermionic emitter and feature of a thermionic X-ray tube. (b) Schematics of a CNT field electron emitter using a free-standing CNT film and feature of a cold cathode X-ray tube. A low-density and radial-direction electron beam is emitted at the hot filament thermionic emitter. A high-density and vertical-direction electron beam is emitted at the edge of the free-standing SWCNT film of the CNT field electron emitter. (c) Formation of a densely packed SWCNT film prepared using vacuum filtration technique. (d) A lot of quasi-vertically aligned SWCNT tips existed at the edge of the free-standing SWCNT film and schematic of electron emission from the tip of SWCNT bundles. (e) Schematics of a fabrication method of the CNT field electron emitter with a different CNT film length.

fast operation, digital operation, a small focal size, and low power consumption. Diverse approaches to fabricate cold cathode X-ray sources have been studied by adopting field electron emitters using various field emission materials such as semiconductor tips, carbon nanotubes (CNTs), and nano-carbon materials.[1−15] More recently, several research groups reported cold cathode X-ray tubes which can promise potential applications for various X-ray systems even though a history of cold cathode X-ray tubes is only a beginning stage.[16−25] Furthermore, some companies such as Shang Fang, Micro-X, Nanox, and CAT beamtech presented commercial cold cathode X-ray tubes using CNT paste emitters or as-grown CNT emitters or Si tip emitters and started to supply cold cathode X-ray tubes with various specifications in the market. Nevertheless, the cold cathode X-ray tubes still show a relatively low tube current and a large focal spot size, which indicates lower tube performance compared with conventional thermionic X-ray tubes. Therefore, for a daily used X-ray system applications, cold cathode X-ray tubes which have not only a high tube current but also a small focal spot size are inevitably necessary. Nowadays, many studies to realize high-performance cold cathode X-ray tubes are very attractive, and several approaches to fabricate a cold cathode X-ray tube are presented.

CNT materials have been considered as a strong candidate for field electron emission devices due to the excellent electrical, thermal, and mechanical properties of CNTs.[26−29] Since the first report on field emission properties of an individual CNT in 1995, several groups have studied field emission properties of CNTs to investigate the possibility of field emitter applications.[30−35] Along with these efforts, several approaches to fabricating CNT field emitters have been developed, for example, as-grown CNT emitter, electrophoresis CNT emitter, CNT fiber emitter, and sprayed CNT emitter, and CNT paste emitter.[36−42] By the way, the above-mentioned methods have achieved some success such as low turn-on voltage, fast operation, and low power consumption but encountered several requirements about a high emission current, a high emission current density, and long-term emission stability. From these perspectives, a more advanced high-performance CNT field emitter is still needed to be used for practical applications of cold cathode X-ray tubes.

Here, we report a high-performance cold cathode X-ray tube equipped with a CNT field electron emitter made by a free-standing CNT film, demonstrating a high tube current, an

https://doi.org/10.1021/acsnano.2c02233
ACS Nano 2022, 16, 10231−10241

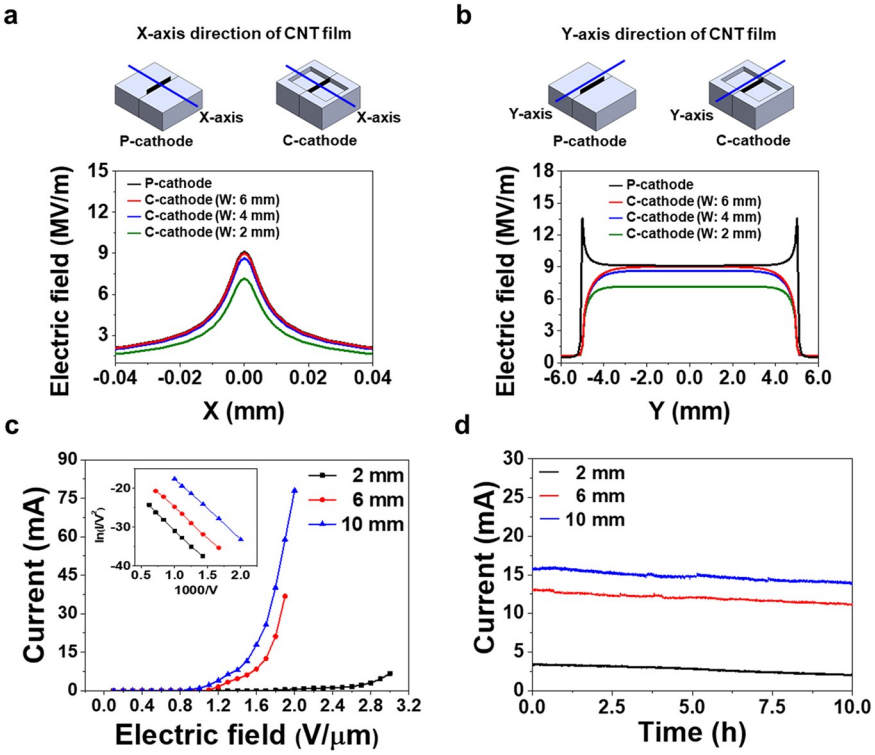

Figure 2. Electric-field distribution and field emission properties of the CNT field electron emitter made by a free-standing CNT film. (a) Simulation results of electric-field distribution along the *x*-axis direction of the CNT film at the CNT field electron emitter. (b) Simulation results of electric-field distribution along the *y*-axis direction of CNT film at the CNT field electron emitter. (c) Electron emission properties of the CNT field electron emitter at a diode configuration. Fowler-Nordheim plots indicates that electron emission exhibits quantum tunneling behavior (inset). (d) Long-term emission stability of the CNT field electron emitter.

extremely high tube current density, a small focal spot size, and good lifetime. Improved performance of our cold cathode X-ray tube is obtained by adopting the CNT field electron emitter and the curve-shape elliptical focusing lens. The unique feature of the CNT field electron emitter made by a free-standing thin CNT film is suitable for achieving both the high tube current and the extremely high tube current density. In addition, the optimized ensemble of the CNT field electron emitter, the slit-shape gate and the curve-shape elliptical focusing lens is appropriate to get a small focal spot size and good lifetime.

RESULTS AND DISCUSSION

The electron emission behavior of the field electron emitter differs from that of a hot-filament thermionic emitter. A thermionic emitter generates a radial electron beam by heating a tungsten filament and a thermionic X-ray tube based on the hot-filament thermionic emitter represents high-temperature operation, a slow response, and an analog response (Figure 1a). By contrast, the field electron emitter generates a directional high-density electron beam through quantum tunneling by applying an electric field and a cold cathode X-ray tube equipped with the CNT field electron emitter presents room-temperature operation, a fast response and a digital response (Figure 1b). The CNT field electron emitter is particularly well suited for a high emission current because of numerous CNT bundles existing at the edge of the CNT film, which can effectively contribute to electron emission. In order to fabricate the CNT field electron emitter, the single-walled CNT (SWCNT) film with a thickness of 7 μm was formed on an anodic aluminum oxide (AAO) membrane using a vacuum filtration process (Figure 1c).[43] A free-standing SWCNT film was subsequently obtained by eliminating the AAO membrane using a 1 M NaOH solution (Supporting Information (SI) Figure S1). The surfactant, sodium dodecyl sulfate (SDS), was removed from the free-standing SWCNT film using isopropyl alcohol (IPA) and the CNT film was densified using ethanol and HNO_3 acid. The free-standing SWCNT film is composed of a highly packed CNT network because of strong van der Waals force between the SWCNTs (SI Figure S2a–d).[44] The prepared free-standing SWCNT film shows high purity and very good crystalline structure (SI Figure S2c–f). The densified free-standing SWCNT film indicates a tensile strength about 40 MPa and a tensile modulus about 2.5 GPa and also shows good mechanical flexibility after bending (SI Figure S2g).[45]

The free-standing SWCNT film was cut using a razor and the vertically aligned tips of SWCNT bundles at the cut edge of the SWCNT film was used for electron emission sites. The key idea for fabricating the CNT field electron emitter is to lift the cut edge of the SWCNT film and use tips of SWCNT bundles at the edge as an electron emission sites (Figure 1d). Scanning electron microscopy (SEM) images show that numerous quasi-vertically aligned SWCNT bundles exist at the edge of the free-standing CNT film. In particular, ethanol and HNO_3 treatment take an important role to densify the free-standing SWCNT film and to form a lot of CNT bundles at the edge of a SWCNT film (Figure 1d). Interestingly, quasi-vertically aligned tips of SWCNT bundles become vertically well aligned after an electrical annealing (SI Figure S4), which can effectively contribute to electron emission. Finally, the

https://doi.org/10.1021/acsnano.2c02233
ACS Nano 2022, 16, 10231–10241

proposed CNT field electron emitter could be simply fabricated by clamping the free-standing CNT film between cathode metal plates (Figure 1e). In this fabrication method, the number of emission sites at the CNT field electron emitter was simply controlled by adjusting the length or the width of the free-standing CNT film (Figure 1e). In addition, by inserting multiple CNT films with identical dimensions between cathode metal plates, an array-type CNT field electron emitter can be also easily fabricated, which can dramatically increase the emission current (SI Figure S3).

The CST program was used to investigate the electric-field distribution along the *x*-axis direction of the CNT field electron emitter (Figure 2a). The electric field is well concentrated on the CNT film for both a planar-type cathode (P-cathode) and a cavity-type cathode (C-cathode). The electric field increases in strength with increasing a cavity width of the C-cathode; however, it saturates at a cavity width of 6 mm. The electric-field distribution at the CNT field electron emitter was also investigated along the *y*-axis direction of the CNT field electron emitter (Figure 2b). For the P-cathode, the electric field is strongly enhanced at the two sides of the edge of the CNT film because of the edge electric-field effect. Sometimes it makes an electrical arcing between the CNT film and the gate electrode in a triode configuration. However, for the C-cathode, the electric field is uniformly distributed over the CNT film, with no edge electric-field effect. Obtained simulation results indicate that the C-cathode with 4 mm cavity width is appropriate to get uniform and strong electric field at the CNT field electron emitter. Potential distribution between the CNT field electron emitter and the anode was evaluated according to the cavity width of the cathode (SI Figure S5). Simulation result shows that potential at the CNT field electron emitter in the *x*-axis direction becomes higher as the cavity width of the cathode increases but it saturates over the cavity width of 4 mm. On the other hand, potential distribution at the CNT field electron emitter in the *y*-axis direction is almost same regardless of the cavity width. It is well understood that potential distribution of the CNT field electron emitter is also very uniform when a cavity width at the C-cathode is over 4 mm.

Based on simulation results, the CNT field electron emitter was fabricated on the C-cathode with 4 mm cavity width and its electron emission properties were quantitatively characterized by measuring the emission current in a diode configuration (Figure 2c). The current−electric field (*I*−*E*) curve indicates that both the turn-on electric field (corresponding to 0.1 μA emission current) and the threshold electric field (corresponding to 1.0 mA emission current) decrease with increasing length of the CNT film. In fact, the turn-on electric field is 1.34 V/μm, 0.79 V/μm, and 0.75 V/μm at CNT film lengths of 2 mm, 6 mm, and 10 mm, respectively, and the threshold electric field of the CNT field electron emitter is 2.31 V/μm, 1.18 V/μm, and 1.04 V/μm at CNT film lengths of 2 mm, 6 mm, and 10 mm, respectively. The emission current of the CNT field electron emitter rapidly increases with increasing length of the CNT film. The emission current of the CNT field electron emitter is 6.7 mA, 36.9 mA, and 78.6 mA at an emitter length of 2 mm, 6 mm, and 10 mm, respectively. It is noteworthy that the emission current of the CNT field electron emitter with a 10 mm CNT film length reaches 78.6 mA (equivalent to an emission current density of 112 A/cm^2) at an applied electric field of 2.0 V/μm. This good result is caused by a unique feature of our CNT field electron emitter made by the free-standing CNT film which has a lot of vertically aligned tips at the CNT bundles (SI Figure S4). Those vertically aligned tips at the CNT bundles can effectively contribute electron emission. By the way, the CNT field electron emitter with a 2 mm length indicates a very low emission current. It is caused by a strong screening effect of the electric field at the cavity edge of the C-cathode structure. In general, for various X-ray tube applications, field electron emitter should present not only a high emission current but also a high emission current density. Interestingly, point-type CNT field emitters made by a CNT film or a CNT fiber indicated a much high emission current density but unfortunately showed a low emission current. For example, The CNT film emitter indicated an extremely high emission current density of 1×10^5 A/cm^2 corresponding to a high emission current of 22.4 mA.[43] The CNT fiber with a diameter of 9 μm also showed the extremely high emission current density of 5.8×10^3 A/cm^2, corresponding to the emission current of 3.6 mA.[46] In fact, the point-type CNT field emitter is very useful for high-resolution microscopy or nondestructive analysis or mammography due to both a high emission current density and a small focal spot. However, it has a critical limitation for diverse X-ray applications due to a relatively low emission current. On the other hand, the CNT paste emitter showed a very high emission current of 600 mA but indicated a very low emission current density of 87.5 mA/cm^2 due to a large emission area.[47] The as-grown CNT field emitter also showed a much high emission current of 710 mA but indicated a low emission current density of 3.55 A/cm^2 due to a large emission area.[48] Notably, our CNT field electron emitter indicates not only the high emission current but also the high emission current density, which can be used for a cold cathode X-ray tube to be suitable for various X-ray applications.

Fowler−Nordheim (F−N) plots was calculated on the basis of the measured emission current. F−N plots reveal that the electron emission basically follows quantum tunneling behavior at the CNT field electron emitter (Inset of Figure 2c). The field enhancement factor obtained from the F−N plots is estimated to be 4167, 4322, and 4521 for a CNT film length of 2 mm, 6 mm, and 10 mm, respectively. Interestingly, the obtained field enhancement factor of the CNT field electron emitter is roughly three to four times greater than that of CNT paste field electron emitters.[49] We consider that it is caused by both the unique morphology of the free-standing CNT film and the high density of the emission sites at the edge of the CNT film. The long-term emission stability of the CNT field electron emitter was investigated in pulsed operating mode. The emission current was evaluated at an applied constant voltage and an initial emission current was started at 3 mA, 13 mA, and 16 mA for the CNT film lengths of 2 mm, 6 mm, and 10 mm, respectively (Figure 2d). In general, the CNT field electron emitter is considered to be acceptable for real applications if a degradation rate of the emission current is below 50% during long-term emission stability test. In this work, the CNT field electron emitter roughly indicates a degradation rate of 15% over 10 h when it starts at a high emission current of 16 mA (corresponding to an emission current density of 22.8 A/cm^2). By the way, both the CNT paste emitter and the as-grown CNT emitter also indicated good long-term emission stability at a high emission current of 600 mA for 7 h and 500 mA for 20 h, respectively.[47,48] But it is noteworthy that our CNT field electron emitter indicates good emission stability at a higher emission current density

https://doi.org/10.1021/acsnano.2c02233
ACS Nano 2022, 16, 10231−10241

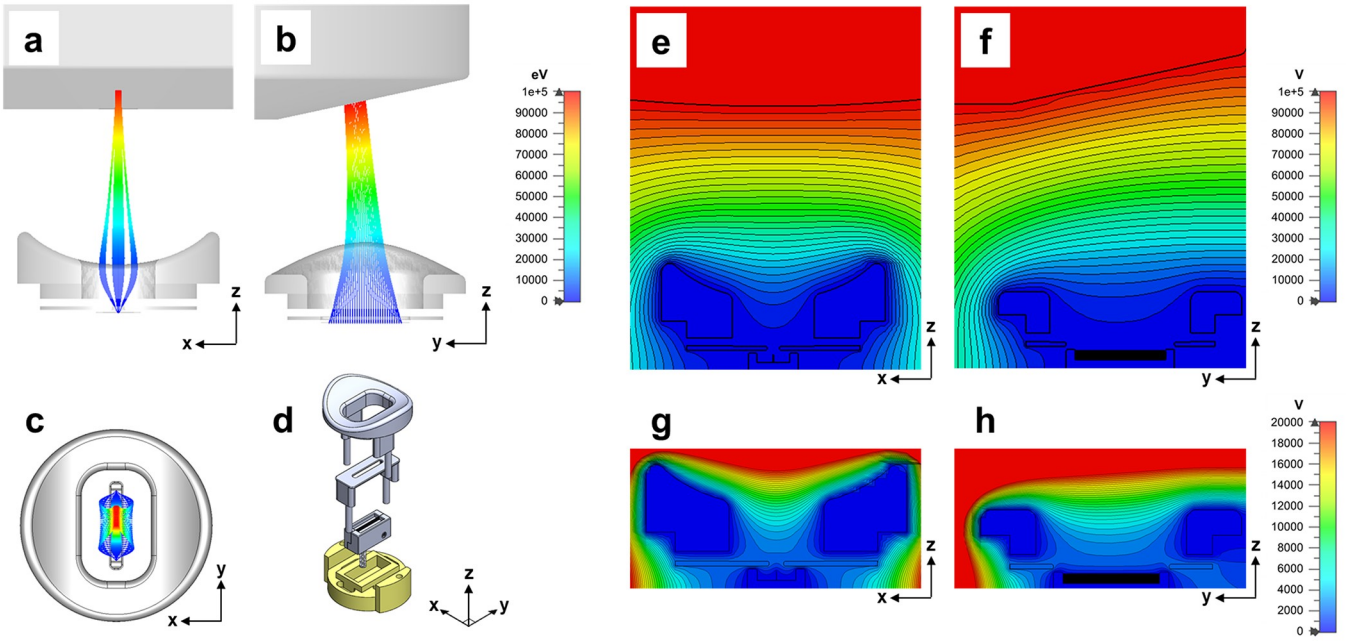

Figure 3. Simulation results of an electron-beam trajectory and potential distribution of the cold cathode X-ray source. (a) A side-view cross-section of an electron-beam trajectory from the CNT field electron emitter to the anode in the *x*-axis direction (a cavity width). (b) A side-view cross-section of an electron-beam trajectory from the CNT field electron emitter to the anode in the *y*-axis direction (a cavity length). (c) A top view of an electron-beam trajectory indicating a high-density electron beam concentrated at a center of the anode. (d) Schematic of an assembly of components of cold cathode X-ray tube such as the ceramic plate, the CNT field electron emitter, the gate and the focusing lens. (e) A side-view cross-section of potential distribution between the focusing lens and the anode in the *x*-axis direction. (f) A side-view cross-section of potential distribution between the focusing lens and the anode in the *y*-axis direction. (g) A side-view cross-section of potential distribution between the CNT field electron emitter and the focusing lens in the *x*-axis direction. (h) A side-view cross-section of potential distribution between the CNT field electron emitter and the focusing lens in the *y*-axis direction.

compared with the CNT paste emitter and the as-grown CNT emitter. It means that our CNT field electron emitter can endure a high emission current load during long-term emission operation. Good emission stability of our CNT field electron emitter is mainly attributed to abundant emission sites at the edge of the free-standing CNT film. An emission current load for each contributing emission sites can be reduced if a CNT field electron emitter has a lot of emission sites. The low emission current load at individual emission sites decreases degradation of tips at the CNT film during field electron emission, resulting in improved long-term emission stability.

The geometry and dimension of components of the cold cathode X-ray tube, which consist of the CNT field electron emitter, the gate electrode and the focusing lens, were designed using the SOLIDWORKS program by evaluating potential distribution and an electron-beam trajectory using the CST program. Understanding of an electron-beam trajectory of the cold cathode X-ray tube is important because X-ray generation is mainly determined by an electron beam density and a focal spot size of electron beam at the anode. The electron beam extracted from the CNT field electron emitter passes through the gate and the focusing lens, and finally arrives at the anode. Therefore, high electron-beam transmittance through the gate is an important issue for increasing the operating stability and lifetime of the cold cathode X-ray tube. A side-view cross-section of an electron-beam trajectory from the CNT electron emitter to the anode is illustrated in the *x*-axis direction and in the *y*-axis direction, respectively (Figure 3a,b). An electron beam with a small focal spot is concentrated at the anode through the curve-shape elliptical focusing lens in the *x*-axis direction. On the other hand, it indicates a relatively large focal spot size in the *y*-axis direction. A top view of an electron-beam trajectory shows that a high-density electron beam is strongly concentrated at a center of the anode (Figure 3c). The focused electron beam is appropriate to realize a small focal spot size at the anode, which in turn leads to a high-resolution X-ray image.

A side-view cross-section of an electron-beam trajectory from the CNT electron emitter to the gate is illustrated in the *x*-axis direction (SI Figure S6). The electron beam is extracted at the edge of the free-standing CNT film by applying the gate voltage and pass through the gate slit, and it arrives at the cavity of the focusing lens. Schematic illustrates an assembled of X-ray source, which is composed of the ceramic plate, the CNT field electron emitter, the gate and the focusing lens (Figure 3d).

A side-view cross-section of potential distribution between the focusing lens and the anode is presented with respect to the *x*-axis direction and *y*-axis direction, respectively (Figure 3e,f). The simulation results show that potential distributed at the cavity center of focusing lens in the *x*-axis direction (cavity width) is stronger than potential distributed in the *y*-axis direction (cavity length). A side-view cross-section of potential distribution between the CNT field electron emitter and the focusing lens is also presented with respect to the *x*-axis direction and *y*-axis direction, respectively (Figure 3g,h). The simulation results between the CNT field electron emitter and the focusing lens also indicate that potential distributed in the *x*-axis direction (cavity width) is stronger at the cavity center of focusing lens than potential in the *y*-axis direction (cavity length). We also evaluated an electron-beam trajectory and potential distribution of the cold cathode X-ray source

https://doi.org/10.1021/acsnano.2c02233
ACS Nano 2022, 16, 10231−10241

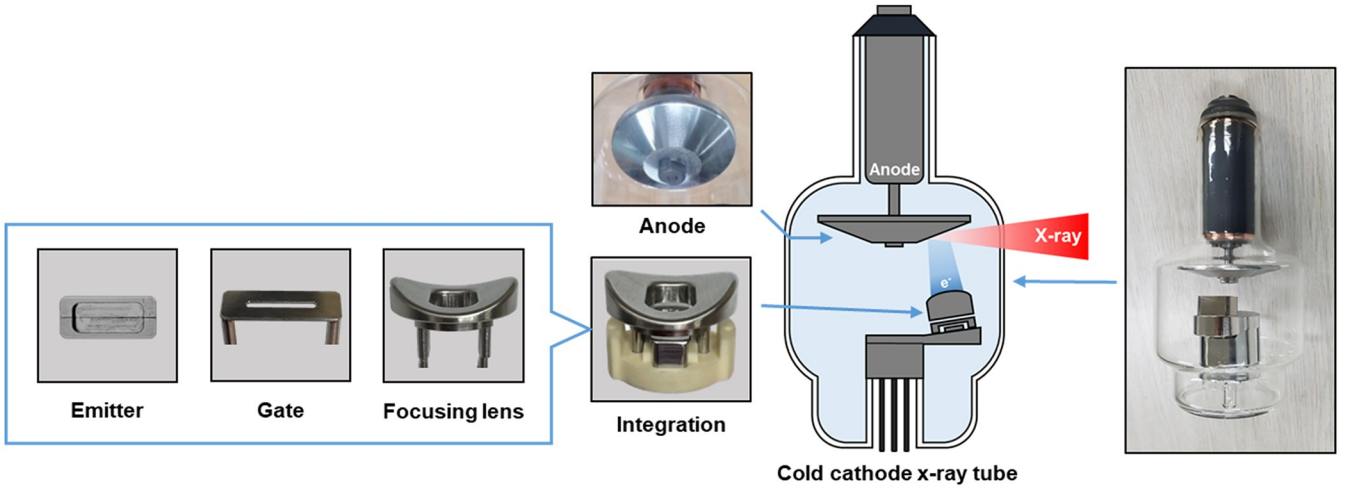

Figure 4. Optical images of key components of the cold cathode X-ray tube and the glass vacuum sealed cold cathode X-ray tube. The cold cathode X-ray tube consists of the CNT field electron emitter, the gate with a slit, the curve-shape elliptical-cavity focusing lens and the rotation-type reflective anode. The schematic of the cold cathode X-ray tube illustrates X-ray generation at the anode by an incident electron beam emitted from the CNT field electron emitter.

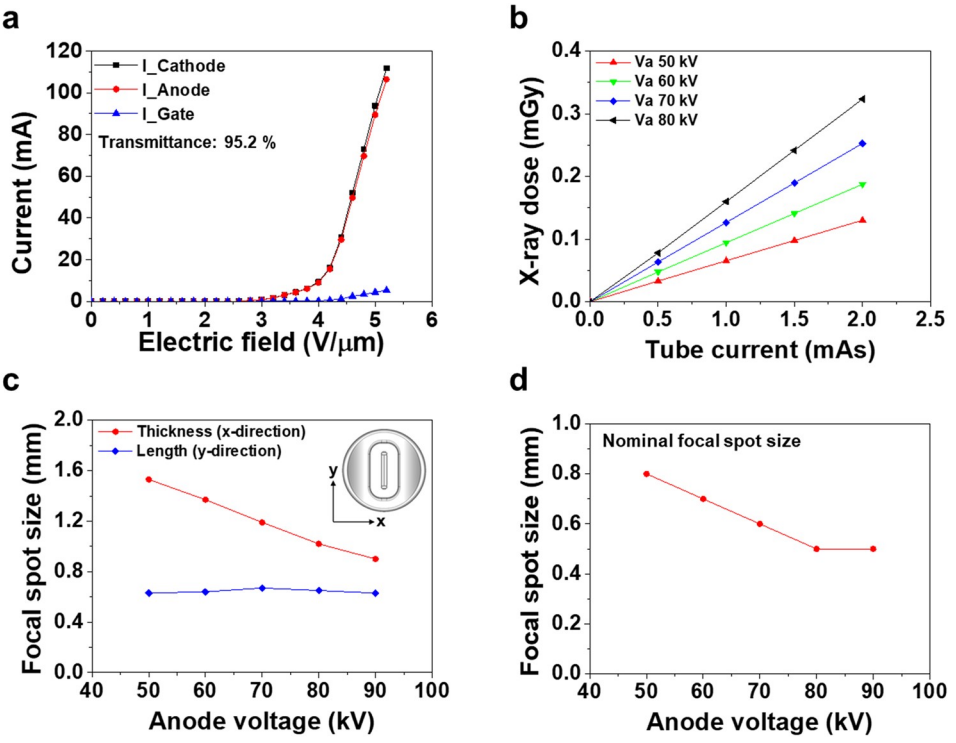

Figure 5. Characterization of the cold cathode X-ray tube. (a) *I*–*V* characteristics of the cold cathode X-ray tube using the CNT field electron emitter made by a free-standing CNT film with a 10 mm length. (b) X-ray dose of the cold cathode X-ray tube dependent on the tube current and the tube voltage. (c) The focal spot size of the cold cathode X-ray tube at a tube current of 100 mA according to a tube voltage. (d) The Nominal focal spot size of the cold cathode X-ray tube according to a tube voltage.

according to the geometry of the focusing lens. Simulation results show that the curve-shape elliptical focusing lens separated with the gate can effectively concentrate the electron beam at the anode compared with the curve-shape elliptical focusing lens connected with the gate or the flat-shape elliptical focusing lens connected with the gate (SI Figure S7 and S8). It is understood that a high-density focused electron beam is important to increase resolution of X-ray images at X-ray tubes. Therefore, the proposed curve-shape elliptical focusing lens separated with the gate is useful for realizing high-performance X-ray tubes (SI Figure S9).

Optical images of key components and the cold cathode X-ray tube are shown (Figure 4). The cold cathode X-ray tube consists of key components such as the CNT field electron emitter, the gate, the curve-shape elliptical focusing lens and the rotation-type reflective anode. To fabricate the cold cathode X-ray tube, four components are assembled and the assembled set is inserted into a glass tube, and finally vacuum sealed to complete the cold cathode X-ray tube. The schematic

https://doi.org/10.1021/acsnano.2c02233
ACS Nano 2022, 16, 10231–10241

of the cold cathode X-ray tube illustrates X-ray generation at the anode by an incident electron beam emitted from the CNT field electron emitter. The CNT field electron emitter is made by a free-standing CNT film with a thickness of 7 μm and a length of 10 mm. The gate has a slit with a width of 1.5 mm and a length of 12 mm. The curve-shape elliptical focusing lens has a cavity width of 8 mm, a cavity length of 18 mm and a cavity height of 5 mm, respectively. The rotation-type reflective anode has a diameter of 3 in. and an angle of 12 degrees. The CNT field electron emitter is separated from the gate using a ceramic spacer with a thickness of 0.5 mm. The gap between the gate and the focusing lens is 1.0 mm, and the gap between the focusing lens and the anode is 20 mm.

Performance of the cold cathode X-ray tube such as a tube current, X-ray dose and a focal spot size was characterized (Figure 5). The cold cathode X-ray tube exhibits the high tube current of 106.4 mA (corresponding to the extremely high tube current density of 152 A/cm^2) at the gate voltage of 2.6 kV and the tube voltage of 80 kV (Figure 5a). Interestingly, our cold cathode X-ray tube shows a very high tube current and an extremely high tube current density due to high electron emission sites at the CNT field electron emitter. Several articles also reported a maximum emission current of an individual SWCNT is about 1 μA.[50] Therefore, emission sites of our CNT field electron emitter can be calculated to be about 106 400 ea. Sometimes, high density emission sites induce screening effect at the field electron emitters.[51] At a higher electric field region, we could find that a gradient of an emission current is slightly decreased. It means that screening effect may occur between the effective emission sites during field electron emission.

It is well-known that X-ray tubes need a high tube current density besides a high tube current for real X-ray system applications because the high tube current density is favorable to get a small focal spot size. Some important results on performance of cold cathode X-ray tube have been reported. Shang Fang company reported CNT paste emitter based cold cathode X-ray tube which has a tube current of 3 mA at a high tube voltage of 180 kV. Nanox company also presented a cold cathode X-ray tube based on Si tip emitters, indicating a tube current of 20 mA (corresponding to a tube current density of ~20 mA/cm^2) at a tube voltage of 40 kV. Recently, Micro-X company reported a cold cathode X-ray tube which has a tube current of 130 mA (corresponding to a tube current density of ~200 mA/cm^2) at a high tube voltage of 110 kV. ETRI group also reported a cold cathode X-ray tube using an array-type CNT paste emitters, which has a tube current of 250 mA (corresponding to a tube current density of 340 mA/cm^2) at a tube voltage of 80 kV.[25] It is still a very difficult mission for CNT cold cathode X-ray tubes to have a high tube current and a high tube current density at the same time. Nevertheless, our cold cathode X-ray tube achieves not only the high tube current but also the extremely high tube current density. In addition, the cold cathode X-ray tube indicates a very high electron-beam transmittance of 95.2% at the electric field of 5.2 V/μm, which is enough high for various X-ray tube applications. The advanced electron-beam transmittance is based on optimized geometries of the CNT field electron emitter using a free-standing thin CNT film and the gate with a slit structure. By optimizing the size of a gate slit (a 1.5 mm width and a 12 mm length), the electron-beam transmittance is much increased. It is considered that the high electron-beam transmittance can increase lifetime of the cold cathode X-ray tube due to reduced degradation of the gate during field emission operation (SI Figure S14). In this work, we found that the tube current of the CNT cold cathode emitter indicates was strongly governed by the gate voltage, whereas the influence of the tube current by the anode voltage was not so strong. The tube current was slightly increased by increasing the anode voltage (SI Figure S10). Based on obtained results, we forecast that our cold cathode X-ray tube with the extremely high tube current density and a very high electron-beam transmittance can possess a good opportunity to be used for various X-ray system applications in the future.

The X-ray dose linearly increases with increasing the tube current and also increases with increasing the tube voltage (Figure 5b). In this work, X-ray dose was measured at a distance of 60 cm from the X-ray tube. Very high-resolution X-ray images of a pig's foot (diameter of 6 cm) are achieved at X-ray dose of below 0.25 mGy (corresponding to 25 mA - 60 ms) in the range of the tube voltage of 50−80 kV (SI Figure S11).

We evaluated the focal spot size using a slit technique measurement (RTI Slit Camera, IEC standard 60336) (SI Figure S12). The focal spot size was measured at the tube current of 100 mA at the tube voltage of 50−90 kV. The calculated focal spot size of the cold cathode X-ray tube is in the range of 1.55 mm ~0.9 mm in the x-axis direction and about 0.6 mm in the y-axis direction, respectively (Figure 5c). In addition, the obtained nominal focal spot size is in the range of 0.5−0.8 mm according to the tube voltage (Figure 5d). The nominal focal spot is increased with decreasing the tube voltage below the tube voltage of 70 kV but an almost same value (0.5 mm) over the tube voltage of 80 kV. Notably, the cold cathode X-ray tubes indicates a very small X-ray focal spot of 0.5 mm over an anode voltage of 80 kV, which is very favorable for attaining high-resolution X-ray images. It is well-known that the focal spot size for daily used X-ray tubes for X-ray CT applications is normally in the range of 0.6−1.2 mm. It means that the focal spot size of our cold cathode X-ray tube is enough high for real applications for X-ray radiography or X-ray CT. We investigated the focal spot size of the cold cathode X-ray tube according to the structure of focusing lens (SI Figure S13). The simulation results show that the optimized structure of focusing lens is very important to get a small focal spot size. The curve-shape elliptical focusing lens separated with the gate shows a smaller focal spot size compared with a flat-shape elliptical focusing lens or a curve-shape focusing lens connected with the gate. We consider that the small focal spot of the cold cathode X-ray tube is mainly attributed to unique features of both the CNT field electron emitter fabricated using a free-standing thin CNT film and the optimized curve-shape elliptical-cavity focusing lens. We also evaluated lifetime of the cold cathode X-ray tube at a tube current of 96 mA and a tube voltage of 80 kV (SI Figure S14). Lifetime of the cold cathode X-ray tube was evaluated at a starting tube current of 96 mA and a tube voltage of 80 kV in pulse operation mode. In this measurement, the pulse operation mode indicates a pulse width of 0.1 ms and a duty cycle of 10% at 1 kHz frequency. The tube current indicates a little fluctuation during field electron emission at a high tube current due to a high burden of an emission current at emission sites but the cold cathode X-ray tube shows a small degradation during 100 000 shots, indicating good lifetime. In means that the cold cathode X-ray tube is an enough high level for real X-ray applications.

Performance of X-ray tubes was evaluated by comparing the tube current density and the focal spot size according to the

https://doi.org/10.1021/acsnano.2c02233
ACS Nano 2022, 16, 10231−10241

electron emitter type (Figure 6). Especially, instead of the tube current, the tube current density was investigated to compare

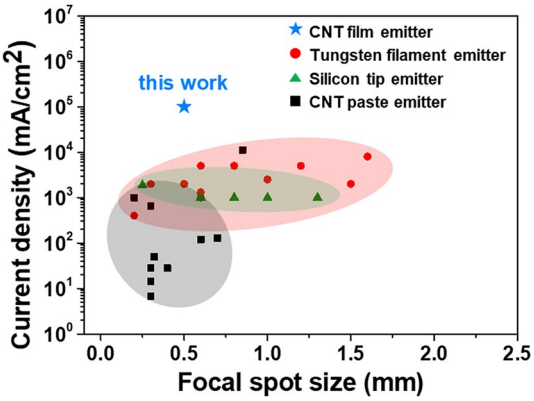

Figure 6. Comparison of performance of X-ray tubes according to various electron emitters.

performance of X-ray tubes because each X-ray tube has a different size or a geometry for application targets. Four kinds of electron emitters such as the CNT emitter using a free-standing CNT film (CNT film emitter), the tungsten filament emitter, the Si tip emitter, and the CNT paste emitter were selected.[2−4,10,11,52−62] From comparison results, it is well understood that our cold cathode X-ray tube shows a much high tube current density at a small focal spot size. By the way, some X-ray tubes indicate a smaller focal spot size than our cold cathode X-ray tube but even though they show a relatively lower tube current.[4,18,24] Such kinds of X-ray tubes can be used for limited X-ray application systems like high-resolution X-ray microscopy or nondestructive analysis or medical mammography due to a small focal spot size. However, the cold cathode X-ray tube should guarantee a high tube current density and a small focal spot size for diverse applications to medical X-ray diagnosis systems like X-ray radiography or X-ray CT.

CONCLUSIONS

The cold cathode X-ray tube was fabricated using the CNT field electron emitter made by a free-standing CNT film. The cold cathode X-ray tube consists of CNT field electron emitter, the gate with a slit, the curve-shape elliptical focusing lens and the rotation-type reflective anode. Our cold cathode X-ray tube indicates not only a high tube current of 106.4 mA but also an extremely high tube current density of 152 A/cm^2 at the tube voltage of 80 kV. The high tube current is mainly attributed to a high density of emission sites at the CNT field electron emitter due to a unique morphology of the free-standing CNT film. Especially, our cold cathode X-ray tube indicates high electron beam transmittance of 95.2%. The cold cathode X-ray tube shows a small focal spot of 0.5 mm at a tube current of 100 mA over a tube voltage of 80 kV and indicates high-resolution X-ray images at a tube current of 25 mA for 60 ms over a tube voltage of 50 kV, respectively. In addition, the cold cathode X-ray tube presents good lifetime during 100 000 shots even though it indicates a little fluctuation due to a high burden of an emission current at emission sites. After all, we consider that high performance of the cold cathode X-ray tubes is based on an ensemble of the CNT field electron emitter, the gate with a slit and the curve-shape elliptical focusing lens. Due to obtained results of the cold cathode X-ray tube, we believe that the proposed cold cathode X-ray tube can pave a new path to the development of future X-ray sources for portable and mobile X-ray medical systems, advanced X-ray CT systems without a gantry and security check X-ray systems in the future.

METHODS

Materials and Preparation of a Free-Standing CNT Film. Single-walled carbon nanotubes (SWCNT) were synthesized using arc-discharge. The SWCNTs were purified using thermal annealing at 400 °C for 30 min at the furnace in ambient air and HCl treatment for 1 h. Finally, the purified SWCNTs were thermally annealed at 900 °C for 1 h at a vacuum furnace. A CNT film was fabricated on an anodized aluminum oxide (AAO) membrane from a CNT solution using a vacuum filtration method. The CNT solution was prepared by dispersing SWCNT powder in a 0.1 wt % sodium dodecyl sulfate (SDS) solution using ultrasonication and centrifugation processes. A free-standing CNT film was obtained after the AAO membrane was removed using a 1 M NaOH solution. The CNT film was cleaned by removing SDS from the surface of the CNT film using deionized (DI) water. The free-standing CNT film was densified by treatment with an ethanol solution and a diluted nitric acid solution in sequence. After cleaning with DI water, it was dried in an oven at 100 °C in ambient air. The free-standing CNT film exhibited a highly packed CNT network, and the thickness of the CNT film was about 7 μm.

Fabrication of the CNT Field Electron Emitter. The free-standing SWCNT film was cut using a razor, and it was inserted between stainless steel (SUS 304) plates and clamped to fabricate the CNT field electron emitter. Observation of the edge of the free-standing SWCNT film indicated that numerous CNT bundles were evenly distributed at the edge of the CNT film. The CNT bundles at the edge of SWCNT film contribute to electron emission under an applied electric field. The number of emission sites at the CNT field electron emitter was easily controlled by adjusting the length of the free-standing SWCNT film.

Fabrication of the Cold Cathode X-ray Tube. The cold cathode X-ray tube was composed of four components such as the cathode, the CNT field electron emitter, the gate, the focusing lens and the reflective anode. The cathode was fabricated by forming a cavity with a width of 4 mm and a length of 10 mm using SUS 304. The CNT field electron emitter was fabricated using a free-standing thin CNT film with a thickness of 7 μm and a length of 10 mm. The gate was fabricated by opening a slit with a width of 1.5 mm and a length of 12 mm at the SUS plate with a thickness of 1.0 mm. The gap between the CNT field electron emitter and the gate was 0.5 mm. The focusing lens was also fabricated by opening a cavity at the SUS cylindrical structure with an elliptical shape and was a curved shape at the side faced to the anode. The focusing lens has a cavity width of 10 mm, a cavity length of 18 mm, and a cavity height of 5 mm. The gap between the gate and the focusing lens was 1.0 mm. The geometries of the cathode, the gate and the focusing lens were designed using SOLIDWORKS Professional 2018 (DASSAULT SYSTEMS). The anode made by composition of W−Ru alloy was reflective and a rotation-type. The gap between the focusing lens and the anode was 20 mm. After assembling the CNT field electron emitter, the gate, the focusing lens and the anode, the assembled set (i.e., the cold cathode X-ray source) was inserted into a glass tube. The assembled set is thermally annealed at 400 °C for 10 h under ambient vacuum of 2×10^{-8} Torr and then electrically annealed at the tube current of 30 mA and the tube voltage of 30 kV for 10 min five times under ambient vacuum of 2×10^{-8} Torr. After the electrical annealing, the glass tube was finally vacuum-sealed by a tip-off process at a vacuum pressure of 2×10^{-8} Torr.

Simulation of the Electric-Field Distribution and Electron-Beam Trajectory. The electric-field distribution at the CNT field electron emitter, the electron-beam trajectory and potential distribution through the focusing lens were simulated was evaluated using CST STUDIO SUITE 2019 (DASSAULT SYSTEMS). The simulation was conducted by adopting following conditions. The

https://doi.org/10.1021/acsnano.2c02233
ACS Nano 2022, 16, 10231−10241

CNT emitter has a thickness of 7 μm and a length of 10 mm, and the cathode has a width of 6 mm and a length of 14 mm. The gate has a width of 8 mm and a length of 21 mm, and the slit of the gate has a width of 1.5 mm and a length of 12 mm. The focusing lens has a diameter of 27 mm and a height of 5.5 mm, and the inner cup of the focusing lens has a width of 10 mm and a length of 16 mm. The gap between the anode and the focusing lens is 19 mm, the gap between the gate and focusing lens is 1 mm and the gap between the gate and the cathode is 0.5 mm. In this work, simulation of electron beam trajectory is conducted at the focusing voltage of 0 V (ground), the anode voltage of 80 kV, the gate voltage of 2500 V and the cathode voltage of 0 V (ground). The initial velocity of an electron is 1.64483 $\times 10^8$ m/s and time is 4.77082 $\times 10^{-7}$ ms.

Characterization of SWCNT Films. The morphology and structure of the free-standing SWCNT film were characterized by field-emission scanning electron microscopy (FESEM, Hitachi S-4700) and high-resolution transmission electron microscopy (HRTEM, FEI TECNAI G2 F30ST), respectively. The crystallinity and purity of the CNTs were investigated by Raman spectroscopy (Horiba Jobin-Yvon LabRAM HR-800) using Ar^+-ion laser excitation (laser-beam wavelength: 514.5 nm) and by thermogravimetric analysis (TGA, TA Instruments TGA-Q50).

Measurement of Field Emission Properties of CNT Field Electron Emitter and Characterization of the Cold Cathode X-ray Tube. The field emission current was measured using a Keithley 2400 source meter unit and a TECHNIX SR15-P-3000 DC voltage source for a diode configuration. The emission current was measure in DC mode in a diode configuration with the voltage seeping rate of 100 V/step. The gap between the emitter and the anode was 1 mm. Long-term emission stability of the CNT field emitter was investigated in pulse mode with a frequency of 1 kHz and a duty of 10%. It also was measure at an emission current of 15 mA for 10 mm CNT film for 10 h in a diode configuration. The field emission current was measured using a Keithley 2290 source meter unit, Spellman SL1200 power supply, and Tektronix AFG3011C function generator for a triode configuration. The gap between the CNT field emitter and the gate was 0.5 mm, the gap between the gate and the focusing lens was 1.0 mm and the gap between the focusing lens and the anode electrode was 20 mm. The anode voltage was as high as 80 kV. Field emission patterns were obtained for an emission current of 1 mA at a diode configuration, and a phosphor-coated ITO glass (anode) was separated by 1 mm from the CNT emitter tip. All measurements were performed at room temperature. In this work, lifetime test of the X-ray tube was measured at an anode current of 20 mA and an anode voltage of 60 kV during 120 000 shots. The pulse operation mode indicates a pulse width of 0.1 ms and a duty cycle of 10% at 1 kHz frequency. The tube current of the cold cathode X-ray tube was measured in pulse mode using active current control (ACC) unit including FET at cathode. By connecting a transistor to the cathode, the pulse waveform (frequency 1 kHz, duty 10%) was applied to the transistor by function generator (generally used cathode current control method). We measured the emission current by checking the Cursor RMS value through the oscilloscope on the cathode. X-ray images were obtained by a DR detector (DRTECH, EVS3643). The focal spot size was calculated using a slit technique measurement (RTI Slit Camera, IEC standard 60336). X-ray dose was measured using an X-ray dosimeter (IBA dosimetry, MagicMaX RQA detector).

ASSOCIATED CONTENT

Supporting Information

The Supporting Information is available free of charge at https://pubs.acs.org/doi/10.1021/acsnano.2c02233.

Fabrication of a free-standing SWCNT film for the CNT field electron emitter; characteristics of the free-standing SWCNT film formed using vacuum filtration process; fabrication and electron emission patterns of the CNT field electron emitter; morphology of tips of SWCNT bundles at the edge of the free-standing SWCNT film; simulation result of potential distribution at the CNT field electron emitter; simulation results of an electron-beam trajectory and potential distribution at the flat-shape elliptical focusing lens; simulation results of an electron-beam trajectory and potential distribution at the curve-shape elliptical focusing lens; simulation results of an electron-beam trajectory and the focal spot size dependent on geometry of the focusing lens; Measurement of the focal spot size using slit technique with RTI Slit Camera (IEC standard 60336); comparison of the focal spot size and resolution of a slit obtained using slit technique with RTI Slit Camera (IEC standard 60336) according to the structure of focusing lens; X-ray images of pig's foot obtained by the cold cathode X-ray tube according to the tube voltage; lifetime test of the cold cathode X-ray tube using the CNT field electron emitter (PDF)

Movie S1. Mechanically stable and flexible free-standing SWCNT film after bending cycle (AVI)

AUTHOR INFORMATION

Corresponding Author

Cheol Jin Lee − *School of Electrical Engineering, Korea University, Seoul 02841, Republic of Korea;* orcid.org/0000-0001-8850-8981; Email: cjlee@korea.ac.kr

Authors

Jun Soo Han − *School of Electrical Engineering, Korea University, Seoul 02841, Republic of Korea*

Sang Heon Lee − *School of Electrical Engineering, Korea University, Seoul 02841, Republic of Korea*

Hanbin Go − *School of Electrical Engineering, Korea University, Seoul 02841, Republic of Korea*

Soo Jin Kim − *School of Electrical Engineering, Korea University, Seoul 02841, Republic of Korea;* orcid.org/0000-0001-7445-2454

Jun Hong Noh − *School of Civil, Environmental and Architectural Engineering, Korea University, Seoul 02841, Republic of Korea;* orcid.org/0000-0002-1143-5822

Complete contact information is available at: https://pubs.acs.org/10.1021/acsnano.2c02233

Author Contributions

[§]J.S.H. and S.H.L. contributed equally to this work. C.J.L. proposed, designed, and supervised the fabrication and characterization of the cold cathode X-ray tube. J.S.H. designed and fabricated the CNT field emitter, the gate electrode and the focusing lens. S.H.L. fabricated and characterized the cold cathode X-ray tube. H.G. prepared and characterized CNT materials. S.J.K. discussed and validated the simulation results of CNT field emitters. J.H.N. discussed data analysis in this work. All authors contributed to discussions about the manuscript.

Notes

The authors declare no competing financial interest.

ACKNOWLEDGMENTS

This work was financially supported by National Research Foundation of Korea (NRF) grant (NRF-2019R1A2C2010267) and Research fund of Korea University. We thank J.-W. Park, C.-H. Kang, and S.-H. Lee (Anam Hospital, Korea University) for X-ray image analysis and A.

https://doi.org/10.1021/acsnano.2c02233
ACS Nano 2022, 16, 10231−10241

Nojeh (The University of British Columbia) for discussion of field emission properties.

REFERENCES

(1) Sugie, H.; Tanemura, M.; Filip, V.; Iwata, K.; Takahashi, K.; Okuyama, F. Carbon nanotubes as electron source in an x-ray tube. *Appl. Phys. Lett.* **2001**, *78*, 2578−2580.
(2) Yue, G. Z.; Qiu, Q.; Gao, B.; Cheng, Y.; Zhang, J.; Shimoda, H.; Chang, S.; Lu, J. P.; Zhou, O. Generation of continuous and pulsed diagnostic imaging x-ray radiation using a carbon-nanotube-based field-emission cathode. *Appl. Phys. Lett.* **2002**, *81*, 355−357.
(3) Zhang, J.; Yang, G.; Cheng, Y.; Gao, B.; Qiu, Q.; Lee, Y. Z.; Lu, J. P.; Zhou, O. Stationary scanning x-ray source based on carbon nanotube field emitters. *Appl. Phys. Lett.* **2005**, *86*, 184104.
(4) Liu, Z.; Zhang, J.; Yang, G.; Cheng, Y.; Zhou, O.; Lu, J. Development of a carbon nanotube based microfocus x-ray tube with single focusing electrode. *Rev. Sci. Instrum.* **2006**, *77*, 054302.
(5) Kawakita, K.; Hata, K.; Sato, H. Development of microfocused x-ray source by using carbon nanotube field emitter. *J. Vac. Sci. Technol. B* **2006**, *24*, 950−952.
(6) Colon, X. C.; Geng, H.; Gao, B.; An, L.; Cao, G.; Zhou, O. A carbon nanotube field emission cathode with high current density and long-term stability. *Nanotechnology* **2009**, *20*, 325707.
(7) Heo, S. H.; Kim, H. J.; Ha, J. M.; Cho, S. O. A vacuum-sealed miniature X-ray tube based on carbon nanotube field emitters. *Nanoscale Res. Lett.* **2012**, *7*, 258.
(8) Ryu, J. H.; Kang, J. S.; Park, K. C. Carbon Nanotube Electron Emitter for X-ray Imaging. *Mater.* **2012**, *5*, 2353−2359.
(9) Iwai, Y.; Koike, T.; Hayama, Y.; Jouzuka, A.; Nakamura, T.; Miyoshi, M.; Minura, H. X-ray tube with a graphite field emitter inflamed at high temperature. *J. Vac. Sci. Technol. B* **2013**, *31*, 02B106.
(10) Jeong, J.-W.; Kim, J.-W.; Kang, J.-T.; Choi, S.; Ahn, S.; Song, Y.-H. A vacuum-sealed compact x-ray tube based on focused carbon nanotube field-emission electrons. *Nanotechnology* **2013**, *24*, 085201.
(11) Lei, W.; Zhu, Z.; Liu, C.; Zhang, X.; Wang, B.; Nathan, A. High-current field-emission of carbon nanotubes and its application as a fast-imaging X-ray source. *Carbon* **2015**, *94*, 687−693.
(12) Chen, D.; Song, X.; Zhang, Z.; Li, Z.; She, J.; Deng, S.; Xu, N.; Chen, J. Transmission type flat-panel X-ray source using ZnO nanowire field emitters. *Appl. Phys. Lett.* **2015**, *107*, 243105.
(13) Gupta, A. P.; Park, S.; Yeo, S. J.; Jung, J.; Cho, C.; Paik, S. H.; Park, H.; Cho, Y. C.; Kim, S. H.; Shin, J. H.; Ahn, J. S.; Ryu, J. Direct synthesis of carbon nanotube field emitters on metal substrate for open-type x-ray source in medical imaging. *Mater.* **2017**, *10*, 878.
(14) Liu, P.; Zhou, D.; Zhang, C.; Wei, H.; Yang, X.; Wu, Y.; Li, Q.; Liu, C.; Du, B.; Liu, L. Crystalline multiwall carbon nanotubes and their application as a field emission electron source. *Nanotechnology* **2018**, *29*, 345601.
(15) Serbun, P.; Porshyn, V.; Bandurin, D.; Lutzenkirchen-Hecht, D. Field emission and electron energy distributions from point-type triangular-shaped emitters made of thin graphene films. *Int. J. Appl. Phys.* **2020**, *127*, 185302.
(16) Shan, J.; Tucker, A. W.; Lee, Y. Z.; Heath, M. D.; Wang, X.; Foos, D. H.; Lu, J.; Zhou, O. Stationary chest tomosynthesis using a carbon nanotube x-ray source array: a feasibility study. *Phys. Med. Biol.* **2015**, *60*, 81−100.
(17) Puett, C.; Inscoe, C.; Hartman, A.; Calliste, J.; Franceschi, D. K.; Lu, J.; Zhou, O.; Lee, Y. Z. An update on carbon nanotube-enabled X-ray sources for biomedical imaging. *WIREs Nanomed Nanobiotechnol* **2018**, *10*, e1475.
(18) Park, S.; Kang, J.-T.; Jeong, J.-W.; Kim, J. W.; Yun, K. N.; Jeon, H.; Go, E.; Lee, J.-W.; Ahn, Y.; Yeon, J.-H.; Kim, S.; Song, Y.-H. A Fully Closed Nano-Focus X-Ray Source With Carbon Nanotube Field Emitters. *IEEE Electron Device Lett.* **2018**, *39*, 1936−1939.
(19) Hong, J. H.; Kang, J. S.; Park, K. C. Fabrication of a compact glass-sealed x-ray tube with carbon nanotube cold cathode for high-resolution imaging. *J. Vac. Sci. Technol. B* **2018**, *36*, 02C109.
(20) Lim, J.; Gupta, A. P.; Yeo, S. J.; Mativenga, M.; Kong, M.; Cho, C. G.; Ahn, J. S.; Kim, S. H.; Ryu, J. Design and fabrication of CNT-based e-gun using stripe-patterned alloy substrate for X-ray applications. *IEEE Trans. Electron Devices* **2019**, *66*, 5301−5304.
(21) Spronk, D.; Luo, Y.; Inscoe, C. R.; Lee, Y. Z.; Lu, J.; Zhou, O. Evaluation of carbon nanotube x-ray source array for stationary head computed tomography. *Med. Phys.* **2021**, *48*, 1089.
(22) Cao, X.; Zhang, G.; Zhao, Y.; Xu, Y.; She, J.; Deng, S.; Xu, N.; Chen, J. Fully vacuum-sealed addressable nanowire cold cathode flat-panel x-ray source. *Appl. Phys. Lett.* **2021**, *119*, 053501.
(23) Gupta, A. P.; Choi, J.; Mativenga, M.; Park, K.; Jang, J.; Yeo, S. J.; Jung, J.; Chae, M. S.; Lee, B. N.; Jang, J.; Zhu, H. L.; Mok, H. S.; Ahn, J. S.; Ryu, J. Compact X-Ray Tube With Ceramic Vacuum Seal for Portable and Robust Dental Imaging. *IEEE Trans. Electron Devices* **2021**, *68*, 4705−4710.
(24) Gupta, A. P.; Yeo, S. J.; Jang, J.; Jung, J.; Choi, J.; Lim, J.; Kim, W.; Park, J.; Park, H.; Chae, M. S.; Yeon, Y. H.; Ahn, J. S.; Kim, S. H.; Kim, N.; Ko, B.; Ryu, J. Development of microfocus x-ray source based on CNT emitter for intraoperative specimen radiographic system. *Proceedings of SPIE, the international society for optics and photonics*, Virtual conference, California, USA, February 15−10; 2021; 115953J.
(25) Kang, J.-T.; Jeong, J.-W.; Park, S.; Kim, J.-W.; Yun, K. N.; Go, E.; Lee, J.-W.; Jeon, H.; Ahn, Y.; Yeon, J.-H.; Kim, S.; Song, Y.-H. Ultra-short, high-dose rate digital x-ray tube based on carbon nanotube emitters for advanced cone-beam breast computed tomography. *Proceedings of SPIE, the international society for optics and photonics*, Town and Country Resort & Convention Center, San Diego, California, USA, February 16−21, 2019; 109481I.
(26) White, C. T.; Todorov, T. N. Carbon nanotubes as long ballistic conductors. *Nature* **1998**, *393*, 240−242.
(27) Kim, P.; Shi, L.; Majumdar, A.; McEuen, P. L. Thermal Transport Measurements of Individual Multiwalled Nanotubes. *Phys. Rev. Lett.* **2001**, *87*, 215502.
(28) Kasumov, A. Yu.; Deblock, R.; Kociak, M.; Reulet, B.; Bouchiat, H.; Khodos, I. I.; Gorbatov, Y. B.; Volkov, V. T.; Journet, C.; Burghard, M. Supercurrents Through Single-Walled Carbon Nanotubes. *Science* **1999**, *284*, 1508−1511.
(29) Treacy, M. M. J.; Ebbesen, T. W.; Gibson, J. M. Exceptionally high Young's modulus observed for individual carbon nanotubes. *Nature* **1996**, *381*, 678−680.
(30) Rinzler, A. G.; Hafner, J. H.; Nikolaev, P.; Nordlander, P.; Colbert, D. T.; Smalley, R. E.; Lou, L.; Kim, S. G.; Tomanek, D. Unraveling Nanotubes: Field Emission from an Atomic Wire. *Science* **1995**, *269*, 1550−1553.
(31) Deheer, W. A.; Bacsa, W. S.; Chatelain, A.; Gerfin, T.; Humphrey-Baker, R.; Forro, L.; Ugarte, D. Aligned Carbon Nanotube Films: Production and Optical and Electronic Properties. *Science* **1995**, *270*, 1179−1180.
(32) Saito, Y.; Hamaguchi, K.; Hata, K.; Uchida, K.; Tasaka, Y.; Ikazaki, F.; Yumura, M.; Kasuya, A.; Nishina, Y. Conical beams from open nanotubes. *Nature* **1997**, *389*, 554−555.
(33) Bonard, J.-M.; Salvetat, J.-P.; Stockli, Y.; De Heer, W. A.; Forro, L.; Chatelain, A. Field emission from single-wall carbon nanotube films. *Appl. Phys. Lett.* **1998**, *73*, 918−920.
(34) Lee, C. J.; Kim, D. W.; Lee, T. J.; Choi, Y. C.; Park, Y. S.; Lee, Y. H.; Choi, W. B.; Lee, N. S.; Park, G.-S.; Kim, J. M. Synthesis of aligned carbon nanotubes using thermal chemical vapor deposition. *Chem. Phys. Lett.* **1999**, *312*, 461−468.
(35) Choi, W. B.; Chung, D. S.; Kang, J. H.; Kim, H. Y.; Jin, Y. W.; Han, I. T.; Lee, Y. H.; Jung, J. E.; Lee, N. S.; Park, G. S.; Kim, J. M. Fully sealed, high-brightness carbon-nanotube field-emission display. *Appl. Phys. Lett.* **1999**, *75*, 3129−3131.
(36) Lee, C. J.; Park, J.; Knag, S. Y.; Lee, J. H. Growth and field electron emission of vertically aligned multiwalled carbon nanotubes. *Chem. Phys. Lett.* **2000**, *326*, 175−180.
(37) Zhang, J.; Tang, J.; Yang, G.; Qiu, Q.; Qin, L.-C.; Zhou, O. Efficient Fabrication of Carbon Nanotube Point Electron Sources by Dielectrophoresis. *Adv. Mater.* **2004**, *16*, 1219−1222.

https://doi.org/10.1021/acsnano.2c02233
ACS Nano 2022, 16, 10231−10241

(38) Wei, Y.; Weng, D.; Yang, Y.; Zhang, X.; Jiang, K.; Liu, L.; Fan, S. Efficient fabrication of field electron emitters from the multiwalled carbon nanotube yarns. *Appl. Phys. Lett.* **2006**, *89*, 063101.
(39) Chen, G.; Shin, D. H.; Roth, S.; Lee, C. J. Field emission characteristics of point emitters fabricated by a multiwalled carbon nanotube yarn. *Nanotechnology* **2009**, *20*, 315201.
(40) Jeong, H. J.; Choi, H. K.; Kim, G. Y.; Song, Y. I.; Tong, Y.; Lim, S. C.; Lee, Y. H. Fabrication of efficient field emitters with thin multiwalled carbon nanotubes using spray method. *Carbon* **2006**, *11*, 2689−2693.
(41) Wei, Y.; Jiang, K.; Liu, L.; Chen, Z.; Fan, S. Vacuum-Breakdown-Induced Needle-Shaped Ends of Multiwalled Carbon Nanotube Yarns and Their Field Emission Applications. *Nano Lett.* **2007**, *7*, 3792−3797.
(42) Kim, Y. C.; Nam, J. W.; Hwang, M. I.; Kim, I. H.; Lee, C. S.; Choi, Y. C.; Park, J. H.; Kim, H. S.; Kim, J. M. Uniform and stable field emission from printed carbon nanotubes through oxygen trimming. *Appl. Phys. Lett.* **2008**, *92*, 263112.
(43) Shin, D. H.; Yun, K. N.; Jeon, S.-G.; Kim, J.-I.; Saito, Y.; Milne, W. I.; Lee, C. J. High performance field emission of carbon nanotube film emitters with a triangular shape. *Carbon* **2015**, *89*, 404−410.
(44) Ruoff, R. S.; Tersoff, J.; Lorents, D. C.; Subramoney, S.; Chan, B. Radial deformation of carbon nanotubes by van der Waals forces. *Nature* **1993**, *364*, 514−516.
(45) Wu, Z.; Chen, Z.; Du, X.; Logan, J. M.; Sippel, J.; Nikolou, M.; Kamaras, K.; Reynolds, J. R.; Tanner, D. B.; Hebard, A. F.; Rinzler, A. G. Transparent, Conductive Carbon Nanotube Films. *Science* **2004**, *305*, 1273−1276.
(46) Behabtu, N.; Yuong, C. C.; Tsentalovich, D. E.; Kleinerman, O.; Wang, X.; Ma, A. W. K.; Bengio, E. A.; ter Waarbeek, R. F.; de Jong, J. J.; Hoogerwerf, R. E.; Fairchild, S. B.; Ferguson, J. B.; Maruyama, B.; Kono, J.; Talmon, Y.; Cohen, Y.; Otto, M. J.; Pasquali, M. Storng, Light, Multifunctional Fibers of Carbon Nanotubes with Ultrahigh Conductivity. *Science* **2013**, *339*, 182−186.
(47) Mihalcea, D.; Faillace, L.; Hartzell, J.; Panuganti, H.; Boucher, S.; Murokh, A.; Piot, P.; Thangaraj, J. C. T. Measurement of Ampère-class pulsed electron beams via field emission from carbon-nanotube cathodes in a radiofrequency gun. *Appl. Phys. Lett.* **2015**, *107*, 033502.
(48) Chen, Z.; Zhang, Q.; Lan, P.; Zhu, B.; Yu, T.; Cao, G.; Engelsen, D. D. Ultrahigh-current field emission from sandwich-grown well-aligned uniform multi-walled carbon nanotube arrays with high adherence strength. *Nanotechnology* **2007**, *18*, 265702.
(49) Choi, Y. C.; Kang, J.-T.; Park, S.; Shin, M.-S.; Jeon, H.; Kim, J.-W.; Jeong, J.-W.; Song, Y.-H. Preparation of a miniature carbon nanotube paste emitter for very high resolution X-ray imaging. *Carbon* **2016**, *100*, 302−308.
(50) Dean, K. A.; Chalamala, B. R. Current saturation mechanisms in carbon nanotube field emitters. *Appl. Phys. Lett.* **2000**, *76*, 375−377.
(51) Nilsson, L.; Groening, O.; Emmenegger, C.; Kuettel, O.; Schaller, E.; Schlapbach, L. Scanning field emission from patterned carbon nanotube films. *Appl. Phys. Lett.* **2000**, *76*, 2071−2073.
(52) Doi, K.; Loo, L.-N.; Chan, H.-P. X-Ray Tube Focal Spot Sizes: Comprehensive Studies of Their Measurement and Effect of Measured Size in Angiography. *Radiology* **1982**, *144*, 383−393.
(53) Kim, J.-W.; Shin, M.-S.; Jeong, J.-W.; Kang, J.-T.; Choi, S.; Park, S.; Yeon, J.-H.; Ahn, S.; Song, Y.-H. Electrostatic Focusing Lens Module with Large Focusing Capability in Carbon Nanotube Emitter-Based X-Ray Sources. *IEEE Electron Device Lett.* **2015**, *36*, 396−398.
(54) Canon Electron Tubes & Devices Co., Ltd. Electron Tubes & Devices Product Catalog. 1385, Shimoishigami, Otawara-shi, Tochigi 324−8550, Japan, 2022.
(55) Siemens Healthineers. OEM X-ray Components. Henkestr. 127, 91052 Erlangen, Germany, 2018.
(56) Schwoebel, P. R.; Boone, J. M.; Shao, J. Studies of a prototype linear stationary x-ray source for tomosynthesis imaging. *Phys. Med. Biol.* **2014**, *59*, 2393−2413.
(57) Poliakine, R.; Ilan, N. Dawn of Digital X-ray Sources: Nano-X Imaging Ltd. Proceedings of RSNA, the radiology society of north america, Virtual conference, November 29 to December 5; 2020.
(58) Qian, X.; Rajaram, R.; Calderon-Colon, X.; Yang, G.; Phan, T.; Lalush, D. S.; Lu, J.; Zhou, O. Design and characterization of a spatially distributed multibeam field emission x-ray source for stationary digital breast tomosynthesis. *Med. Phys.* **2009**, *36*, 4389−4399.
(59) Qian, X.; Tucker, A.; Gidcumb, E.; Shan, J.; Yang, G.; Calderon-Colon, X.; Sultana, S.; Lu, J.; Zhou, O.; Spronk, D.; Sprenger, F.; Zhang, Y.; Kennedy, D.; Farbizio, T.; Jing, Z. High resolution stationary digital breast tomosynthesis using distributed carbon nanotube x-ray source array. *Med. Phys.* **2012**, *39*, 2090−2099.
(60) Kim, H. J.; Kim, H. N.; Raza, H. S.; Park, H. B.; Cho, S. O. An Intraoral Miniature X-ray Tube Based on Carbon Nanotubes for Dental Radiography. *Nucl. Eng. Technol.* **2016**, *48*, 799−804.
(61) Iida, K.; Kenmotsu, H.; Yamazaki, J.; Masuya, H. Devices Having an Electron Emitting Structure. US Patent US10,242,836, field March 14, 2013, and issued March 26, 2019.
(62) Sharma, A.; Kim, H. S.; Kim, D.-W.; Ahn, S. A carbon nanotube field-emission X-ray tube with a stationary anode target. *Microelectron. Eng.* **2016**, *152*, 35−40.

https://doi.org/10.1021/acsnano.2c02233
ACS Nano 2022, 16, 10231−10241